ACADEMIC PRESS

Available online at www.sciencedirect.com
SCIENCE DIRECT®

NeuroImage

NeuroImage 20 (2003) 578–586

www.elsevier.com/locate/ynimg

Rapid Communication

Selective enhancement of functional connectivity in the left prefrontal cortex during sentence processing

Fumitaka Homae,[a,b] Noriaki Yahata,[a] and Kuniyoshi L. Sakai[a,b,*]

[a] *Department of Cognitive and Behavioral Science, Graduate School of Arts and Sciences, The University of Tokyo, Komaba, Tokyo, Japan*
[b] *SORST, Japan Science and Technology Corporation, Kawaguchi-shi, Japan*

Received 27 December 2002; revised 3 April 2003; accepted 24 April 2003

Abstract

We present the results of correlation analyses for identifying temporally correlated activations between multiple regions of interest. We focused on functional connectivity for two regions in the prefrontal cortex: the left inferior frontal gyrus (L. F3t/F3O) and the left precentral sulcus (L. PrCS). Temporal correlations of functional magnetic resonance imaging signals were separately examined during a sentence comprehension task and a lexical decision task, thereby averaging data throughout all voxels within a region of interest used as a reference region. We found that the reciprocal connectivity between L. F3t/F3O and L. PrCS was significantly enhanced during sentence processing, but not during lexico-semantic processing, which was confirmed under both auditory and visual conditions. Furthermore, significantly correlated regions were mostly concentrated in the left prefrontal cortex during the sentence task. These results demonstrate that the functional connectivity within the left prefrontal cortex is selectively enhanced for processing sentences, which may subserve the use of syntactic information for integrating lexico-semantic information.

Keywords: Language; Sentence processing; Syntax; Lexico-semantics; Prefrontal cortex; fMRI; Functional connectivity; Temporal correlations

Introduction

Recent development of neuroimaging techniques, such as functional magnetic resonance imaging (fMRI) and positron emission tomography (PET), has revealed a number of cortical regions with contrasting activations under particular task conditions. In contrast, the use of diffusion tensor imaging (DTI) has provided information on anatomical connectivity in the brain (Conturo et al., 1999; Poupon et al., 2000; Catani et al., 2002). Although these two types of techniques are thought as complementary, the mere combination of these methods does not necessarily lead to the understanding of *functional connectivity* between cortical regions. Given that several cortical regions are activated in a task comparison and that they are anatomically connected, all of their connections are not necessarily functional in that task. In practice, functional connectivity can be regarded as the correlation between signals from different brain regions, which are measured with fMRI and PET, as well as electrophysiological techniques such as electroencephalogram (Horwitz et al., 1992; Friston et al., 1993). To elucidate the true nature of correlated activations, a quantitative and objective method for evaluating functional connectivity needs to be established.

It has recently been shown by Bokde et al. (2001) functional connectivity of the left inferior frontal gyrus and posterior regions is task-dependent during the processing of words and word-like stimuli. In their study, fMRI data from one predefined reference voxel were used for calculating temporal correlations with data from other voxels. However, the data of a single voxel are generally more susceptible to temporal fluctuations than the overall activation of the region of interest (ROI), even if they are spatially smoothed. The presence of noise in certain scanning ses-

* Corresponding author. Department of Cognitive and Behavioral Science, Graduate School of Arts and Sciences, The University of Tokyo, Komaba, 3-8-1 Komaba, Meguro-ku, Tokyo 153-8902, Japan. Fax: +81-3-5454-6261.

E-mail address: sakai@mind.c.u-tokyo.ac.jp (K.L. Sakai).

1053-8119/03/$ – see front matter © 2003 Elsevier Inc. All rights reserved.
doi:10.1016/S1053-8119(03)00272-6

sions may abolish its temporal correlation with other voxels. Moreover, the use of block design, in which one task condition and a control condition are alternated, introduces two different cognitive factors into the results of temporal correlation analyses and thus it is unclear which factor contributes to the connectivity. In another fMRI study, a set of steady-state data for either task runs or resting runs were used to compute temporal correlations, whereas block design data with both task and resting were first used for identifying activated regions (Hampson et al., 2002). The latter data were further used for temporal correlations, after extracting data for each of the two conditions from the block design data. In addition to the iteration procedures using different thresholds for statistical analyses, ROIs of "Broca's area" [Brodmann's areas (BAs) 44 and 45] and "Wernicke's area" (BAs 22 and 39) were identified by a very low threshold of $t = 2$, without addressing the significance of widespread activations. It is thus necessary to establish a method for reliably identifying ROIs and to calculate temporal correlations under a single task condition.

In the present paper, we describe a straightforward method for evaluating functional connectivity, in which only block design data with multiple tasks are used for both the identification of ROIs and the calculation of temporal correlations during a single task. Separate "steady-state" data with a single task are not necessary for the present analysis, because functional localization and connectivity are assessed on the basis of the same block design data. More specifically, we develop a framework of correlation analyses, with which functional connectivity between multiple regions can be examined for a particular task period. This method thus puts a main emphasis on the following two issues in correlation analyses: (1) a ROI functionally defined with task comparisons and (2) temporal correlations between the ROI and other regions under a single task condition. First, we ensure a characterization for the functional role of each ROI with strict task comparisons, and then we average data throughout all voxels within that ROI. Second, the data during a particular task period are extracted from the block design data, thereby minimizing the contribution of different task conditions.

We apply this correlation method for clarifying the functional connectivity among activated regions in the prefrontal cortex as well as other cortical regions, thereby quantifying the functional connectivity that may change according to a specific type of linguistic process. We have recently identified two regions in the prefrontal cortex, which may play critical roles in syntactic processing: the left dorsal prefrontal cortex (L. DPFC; mainly in BA 8), which is close to the left precentral sulcus (L. PrCS), and L. F3op/F3t (pars opercularis and pars triangularis; BAs 44 and 45, across the vertical ramus of the Sylvian fissure) (Embick et al., 2000; Hashimoto and Sakai, 2002; Suzuki and Sakai, 2003). Moreover, an event-related transcranial magnetic stimulation (TMS) study has provided a direct evidence for a causal link between syntactic processing and activity in L. F3op/F3t (Sakai et al., 2002). The fMRI data used for the present analysis were acquired in the experimental paradigm described previously (Homae et al., 2002), in which sentence processing-selective activation was observed in another prefrontal region of L. F3t/F3O (pars triangularis and pars orbitalis; BAs 45 and 47, across the horizontal ramus of the Sylvian fissure). Our current goal is thus to clarify the functional connectivity between these subregions of the left prefrontal cortex during sentence processing.

Materials and methods

Subjects

Ten male native Japanese participated in the experiment (age, 20–27). All subjects showed right-handedness (laterality quotients, 65–100) according to the Edinburgh inventory (Oldfield, 1971). None had a history of neurological or psychiatric diseases. Informed consent was obtained from each subject after the nature and possible consequences of the studies had been explained. Approval for the experiments was obtained from the institutional review board of the University of Tokyo, Graduate School of Arts and Sciences. Data from four of nine subjects in our previous study (Homae et al., 2002), as well as data from six new subjects, were used for the present analysis, which satisfied the selection criteria for head movements (see below). During the fMRI experiments, the task performance of the subjects was evaluated online by LabVIEW software and interface (National Instruments, Austin, TX). For each individual, sessions were discarded if the subject performed at an accuracy rate less than one standard deviation (SD) below the subject's average.

Stimuli and tasks

The stimuli and the experimental design used in the present study were the same as those described previously in detail (Homae et al., 2002). In brief, the same sets of dialogues between two persons in Japanese were used as either auditory or visual stimuli. Using a block design protocol, we tested three types of language tasks: sentence (S) tasks, phrase (P) tasks, and nonword (N_{AV}) tasks. In the S tasks under the auditory (S_A) or visual (S_V) condition, phrases were presented in the order of the original sentences. One phrase in a sentence was randomly replaced with a probe stimulus. These probe stimuli belonged to the same grammatical categories as the phrases they replaced, but were contextually unrelated to the dialogue. The subjects judged whether a probe stimulus was present or not, and responded by pressing one of two buttons. In the P tasks under the auditory (P_A) or visual (P_V) condition, we presented the same phrases used in the S tasks (except probe stimuli), but in a completely randomized order. Because these phrases cannot be integrated into a sentence, auto-

matic sentence processing was prohibited. As a probe stimulus, we randomly replaced a phrase with a pronounceable nonword. In the N_{AV} task, phonologically equivalent nonwords were presented auditorily and visually at the same time, using the same set of the nonwords used in the P tasks. As a probe stimulus, we randomly presented phonologically different nonwords. In a single session (420 s), following the first N_{AV} task block, two sequences of S_A-N_{AV}-P_A-N_{AV} and S_V-N_{AV}-P_V-N_{AV} (N_{AV}, 20 s; S and P, 30 s) were alternated twice. Initiation of each task block was cued by presenting the name of the task on the screen. The choice of S_A or S_V as the first S task block was counterbalanced within a subject.

fMRI data acquisition and analyses

The present study was performed using a 1.5-T MRI system (STRATIS II, Premium; Hitachi Medical Corporation, Tokyo, Japan). With a gradient echo echo-planar imaging (EPI) sequence (TR, 5 s; TE, 50 ms; acquisition time, 2250 ms; flip angle, 90°; field of view, 192 × 192 mm^2; resolution, 3 × 3 mm^2), we scanned over 18 horizontal slices of 4 mm thick, covering the range of $z = -12$ to 60 mm from the AC–PC line. The scanning sounds were confined within the interstimulus interval by using a clustered volume acquisition sequence. In a single scanning session, we obtained 85 volumes following the three dummy images, which allowed for the rise of the BOLD signal. Task specific effects were estimated by following the procedures described in Homae et al. (2002), based on a general linear model (fixed effect model) with a delayed (5-s) boxcar waveform. The significant activation was determined by using the *t* statistics on a voxel-by-voxel basis (corrected $P < 0.05$, with an extent threshold of 19 voxels). For the anatomical identification of significantly activated or correlated regions, we used the Anatomical Automatic Labeling method (Tzourio-Mazoyer et al., 2002).

The functional correlation method

Five preprocessing steps were applied to the data in the following sequence, basically following the operations described by Bokde et al. (2001): (1) the time shifts between slice acquisition in a volume were corrected with statistical parametric mapping software (SPM99; Wellcome Department of Cognitive Neurology, London, UK) in MATLAB (MathWorks, Natick, MA); the functional volume data were further realigned in multiple sessions, and sessions that included data with a translation of more than 1.5 mm in one of the three directions or with a rotation of more than 1.0° were removed; (2) signal values in each volume were normalized to the global mean signal of the volume and multiplied by 1000; (3) using MEDx 3.4.1 (Sensor Systems, Inc., Sterling, VA), low-frequency noise fluctuation was high pass filtered at a cutoff frequency of 0.01 Hz; (4) each individual brain was spatially normalized to the standard brain space as defined by the Montreal Neurological Institute (MNI) by resampling every 3 mm using sinc interpolation and then smoothed with an isotropic Gaussian kernel of 8 mm full width at half maximum; and (5) multiple sessions were collapsed into two sessions for each subject, which were classified according to the choice of S_A or S_V as the first block (the present study was based on fMRI time series data of 12 to 24 sessions per subject). We analyzed both averaged data over the 10 subjects and individual data, to assess potential problems of variable connectivity patterns across subjects (Gonçalves et al., 2001).

The following procedures were employed to evaluate temporal correlations between a ROI and each voxel of all scanned regions. First, we defined a ROI as a cluster of contiguous voxels, within which the cortical region exhibited significant activation in the general linear model analysis of two contrasting tasks. The present analysis is focused on cortical regions involved in sentence processing, and ROIs are defined by comparing the S tasks with the P tasks in each modality of stimulus presentation. The time course of the signal changes in the ROI was represented by averaging the time courses of all the voxels within that ROI. After shifting one time point for a hemodynamic delay, the time course data were segmented into task blocks, and the first time point was removed from six time points in each of S or P blocks for minimizing the effect of hemodynamic changes from the preceding baseline blocks. A task-specific time course was then constructed for each task type by merging the time courses of the corresponding blocks. From the two sets of the time courses (according to the choice of S_A or S_V as the first block), this procedure yielded the S and P task specific time courses containing the block sequences of S_A-S_V-S_A-S_V-S_V-S_A-S_V-S_A and P_A-P_V-P_A-P_V-P_V-P_A-P_V-P_A, respectively. The resultant task-specific time course therefore contained a total of 40 time points. In addition, the time course during the S or P task under each modality condition (S_A, S_V, P_A, and P_V) was constructed with a total of 20 time points. Finally, we evaluated temporal correlations between each voxel of all scanned regions and the predefined ROI. At each voxel, the correlation coefficient with respect to the ROI was calculated between the time course of that voxel and an averaged time course in the ROI. This procedure resulted in a map of temporal correlations for the reference region. The significance of the correlation was tested against the null hypothesis under Student's *t* distribution (Hays, 1994), where the correlation coefficient *r* was converted to the corresponding *t* statistic by

$$t(N-2) = r\sqrt{\frac{N-2}{1-r^2}}$$

on a voxel-by-voxel basis (*N*, the number of time points). For reference, with $N = 40$ and 20, a correlation with $r = 0.5$ corresponds to uncorrected $P = 0.001$ and 0.025 (two-tailed), respectively.

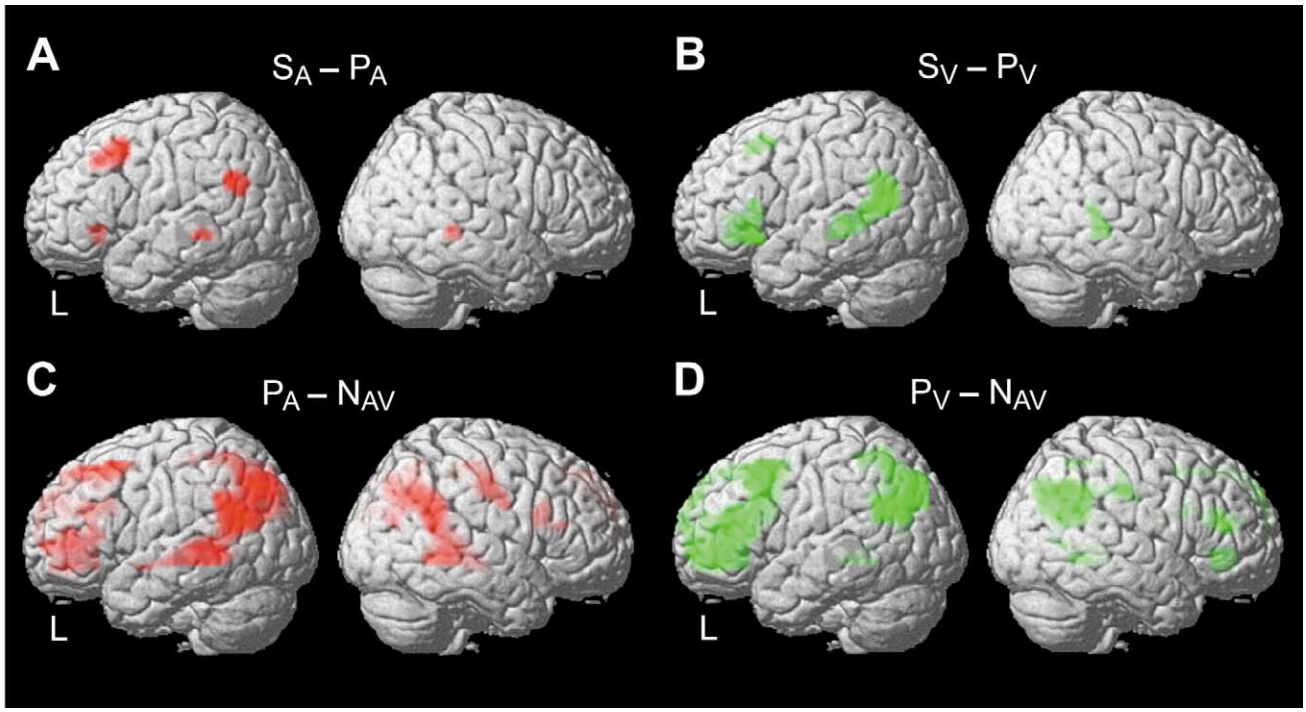

1

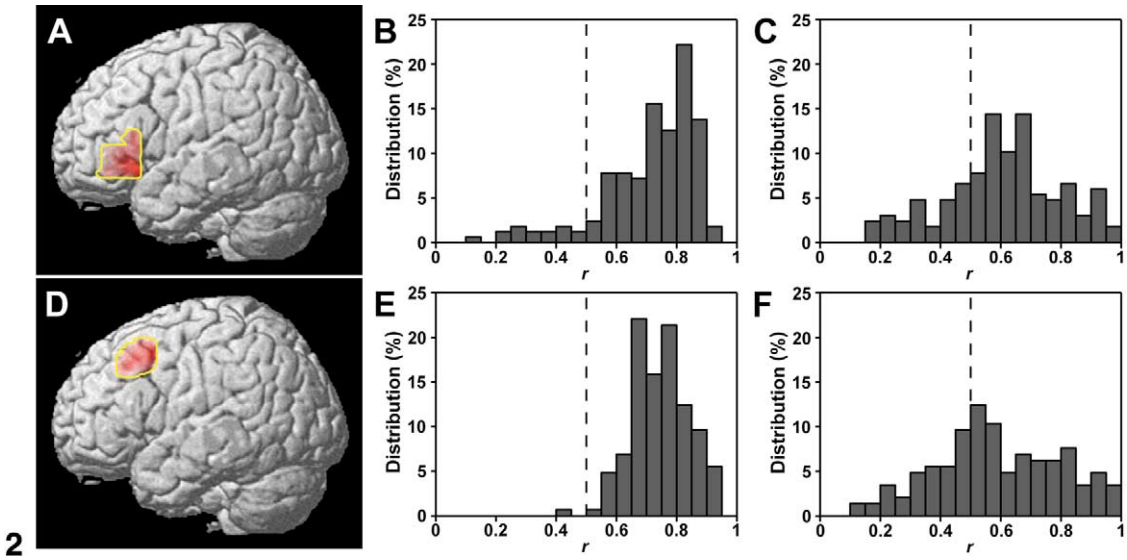

2

Fig. 1. Activated regions in the contrasts S – P and P – N_{AV}. (A and B) Activated regions in S_A–P_A (A) and in S_V–P_V (B) are projected onto a surface rendered representative brain in MNI space. The threshold is set at corrected $P < 0.05$ for the voxel level with an extent threshold of 19 voxels. The left hemisphere (L) is shown to the left. Note that the left inferior frontal gyrus (L. F3t/F3O) and the left precentral sulcus (L. PrCS) show activation in both contrasts. (C and D) Activated regions in P_A–N_{AV} (C) and in P_V–N_{AV} (D) are projected onto a representative brain. In these contrasts, activated regions were found in both hemispheres.

Fig. 2. The functional correlation for the S tasks within L. F3t/F3O or L. PrCS. (A and D) Maps of correlation coefficients (r) between the time course of individual voxels in a region of interest (ROI) and an averaged time course in the ROI are shown in red with yellow boundaries. Selected ROIs are L. F3t/F3O (A) and L. PrCS (D), which contained 167 and 145 voxels, respectively. These regions showed activation in either S_A–P_A or S_V–P_V (Fig. 1). (B and E) Histograms represent the r distribution between the time course of individual voxels in L. F3t/F3O and an averaged time course in L. F3t/F3O (B), and the r distribution between the time courses of individual voxels in L. PrCS and an averaged time course in L. PrCS (E). The broken lines indicate the threshold in correlation analyses ($r = 0.5$). Note that almost all voxels show significant correlations in both regions. (C and F) Histograms represent the r distribution between the time course of individual voxels in L. F3t/F3O and that of a local maximum in L. F3t/F3O (C), and the r distribution between the time course of individual voxels in L. PrCS and that of a local maximum in L. PrCS (F). Note that the overall correlations in (C) and (F) are weaker than those in (B) and (E), respectively.

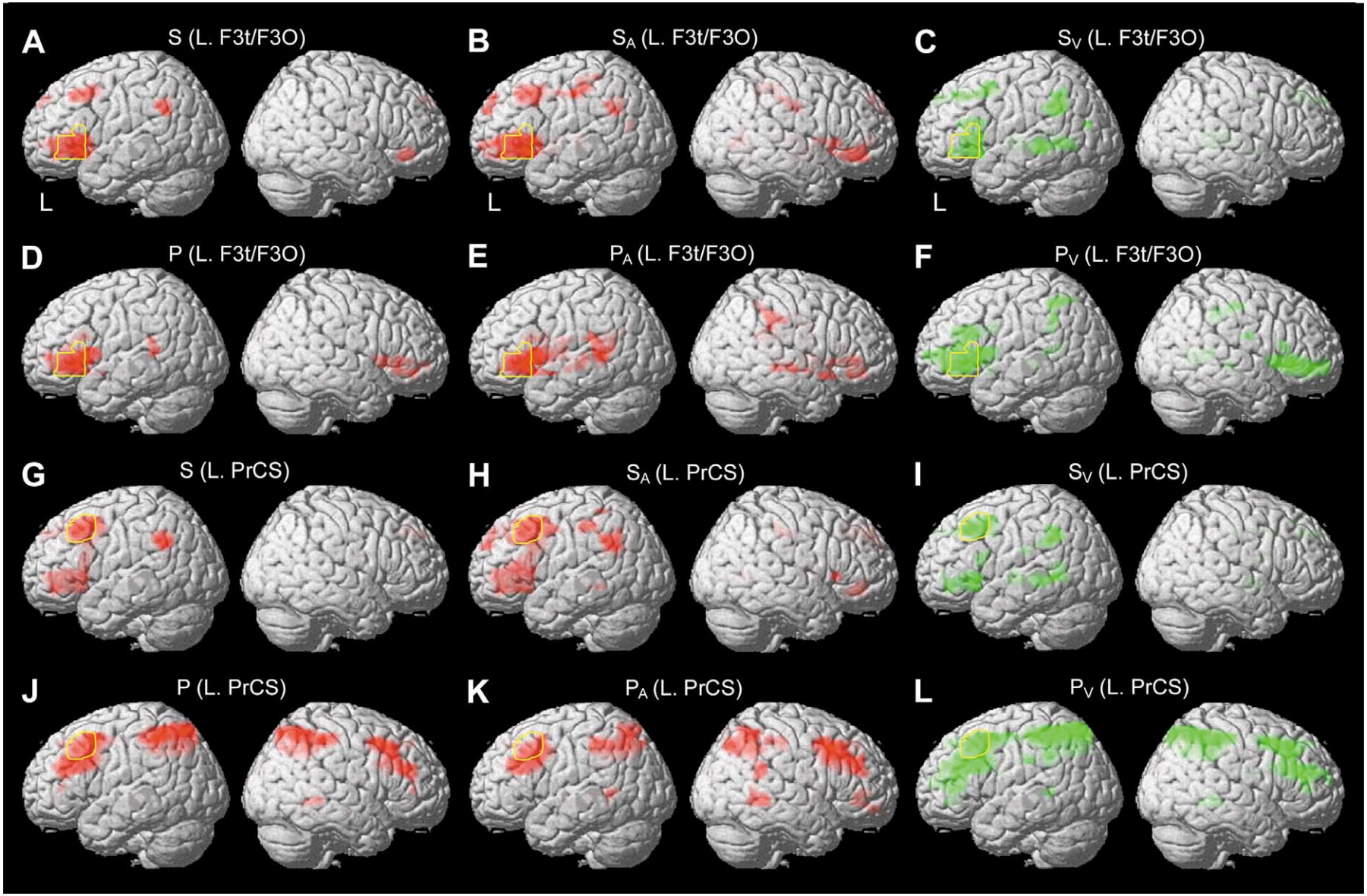

Fig. 3. The functional correlation maps for the S and P tasks. These maps represent cortical regions that show significant temporal correlations ($r > 0.5$) with an extent threshold of 19 voxels, for a reference region (shown with a yellow boundary) of L. F3t/F3O (A–F) or L. PrCS (G–L). These maps are constructed for the S tasks (A–C and G–I) or the P tasks (D–F and J–L), which are based on the time course data under the auditory and visual conditions merged (A, D, G, and J), under the auditory condition alone (B, E, H, and K), or under the visual condition alone (C, F, I, and L). Note that the reciprocal functional connectivity between L. F3t/F3O and L. PrCS is selectively enhanced during the S tasks under both auditory and visual conditions.

Table 1
Activated regions in the S tasks in contrast to the P tasks

Region	BA		Audition: S_A–P_A				Vision: S_V–P_V			
			x	*y*	*z*	*t*	*x*	*y*	*z*	*t*
Inferior frontal gyrus (F3t/F3O)	45/47	L	−51	27	−6	5.7	−45	24	−9	8.4
							−57	24	12	5.6
Precentral sulcus (PrCS)	8	L	−45	15	48	7.6	−42	24	48	5.7
Middle temporal gyrus	21/37	L	−63	−36	−6	5.8	−60	−54	12	7.7
		R	63	−36	−3	5.7	66	−36	−3	6.3
Angular and supramarginal gyrus	39/40	L	−57	−54	27	7.1	−48	−54	30	6.8

Note. Stereotactic coordinates (*x*, *y*, *z*) in Montreal Neurological Institute (MNI) space are shown for each voxel with a local maximum of *t* values in the contrasts indicated ($P < 0.05$, corrected). Abbreviations used for all tables: BA, Brodmann's area; L, left hemisphere; R, right hemisphere; M, medial.

Results and discussion

Task performance

During the fMRI experiments, the performance of the subjects was evaluated online (see Materials and methods): 98.0 ± 1.9, 96.9 ± 1.8, 96.9 ± 2.5, 97.2 ± 1.7, and 92.0 ± 3.0% (mean ± SD) for S_A, S_V, P_A, P_V, and N_{AV} tasks, respectively. An *F* test showed that there was the main effect of tasks in accuracy [$F(4,45) = 11.6$, $P < 0.0001$], and the accuracy for the N_{AV} task was significantly lower than that for the S_A, S_V, P_A, and P_V tasks ($P < 0.0001$). According to an analysis of variance (ANOVA) with two variables [processing (S, P) × modality (audition, vision)], the main effects and the interaction for the four tasks were not significant in accuracy ($P > 0.1$).

ROI analyses

In order to identify cortical regions, which showed more prominent activation in the S tasks than in the P tasks, we directly compared cortical activations in these tasks for each modality condition. The contrasts S_A–P_A and S_V–P_V revealed similar activation patterns (Figs. 1A and B), which were highly lateralized in the left hemisphere. As to the left prefrontal cortex, one ventral region extended from the inferior part of F3t to F3O, across the anterior horizontal ramus of the Sylvian fissure, but not extending to F3op. The other dorsal region in L. PrCS also showed significant activation that mainly located in BA 8. Other activated regions were found in the bilateral middle temporal gyrus (MTG) and in the left angular and supramarginal gyri (L. AG/SMG) (Table 1). The overall patterns of activations replicated those reported previously (Homae et al., 2002). The contrasts P_A–N_{AV} and P_V–N_{AV} also revealed similar activation patterns (Figs. 1C and D; Table 2), which were distributed in both hemispheres. Not all activated voxels of L. F3t/F3O in S_A–P_A and S_V–P_V showed activation in P_A–N_{AV} and P_V–N_{AV}, indicating that it is a sentence processing-selective region.

For the following analyses, two regions in the left prefrontal cortex, L. F3t/F3O and L. PrCS, were selected

Table 2
Activated regions in the P tasks in contrast to the N_{AV} task

Region	BA		Audition: P_A–N_{AV}				Vision: P_V–N_{AV}			
			x	*y*	*z*	*t*	*x*	*y*	*z*	*t*
Inferior frontal gyrus (F3t)	45	L	−45	45	6	8.5	−45	42	3	9.1
		R	57	15	24	6.4	51	36	−3	7.2
			51	30	18	4.9	48	36	15	6.6
Middle frontal gyrus	8	L	−30	21	54	9.5	−24	18	48	9.2
		R					30	18	48	5.2
	10/46	L					−39	57	−6	8.9
Supplementary motor area	6	R	9	−24	54	6.5				
Postcentral gyrus	3/1/2	R	60	−24	54	5.6				
			54	−18	39	6.7				
Superior temporal sulcus	21/22	R	51	−51	21	9.3				
Middle temporal gyrus	21/37	L	−51	−42	0	10.7	−51	−36	−6	6.4
			−54	−30	0	10.7				
Angular and supramarginal gyrus	39/40	L					−54	−54	27	9.7
		R	54	−69	33	9.2	51	−48	24	7.5
							36	−72	39	7.2
Precuneus	7/31	M	−6	−60	39	10.0	−6	−63	39	7.8
Middle occipital gyrus	19	L	−42	−81	36	10.7				

Table 3
Functional connectivity between cortical regions and a left prefrontal region (L. F3t/F3O or L. PrCS) in the S and P tasks

Region	BA		S tasks				P tasks			
			x	*y*	*z*	*r*	*x*	*y*	*z*	*r*
L. F3t/F3O (reference region)										
Inferior frontal gyrus	45/47	R	48	36	−6	0.71	48	42	−9	0.66
(F3t/F3O)							48	30	3	0.67
Inferior frontal gyrus (F3op)	44	L					−48	6	6	0.72
		R					48	15	3	0.65
Precentral sulcus (PrCS)	8	L	−42	15	45	0.80				
Superior frontal gyrus	9/8	M	−3	51	39	0.58				
Superior temporal gyrus	22	L					−57	−42	9	0.57
Supramarginal gyrus	40	L	−60	−51	33	0.70				
			−48	−51	30	0.52				
L. PrCS (reference region)										
Inferior frontal gyrus (F3t/F3O)	45/47	L	−48	42	−6	0.81				
			−48	27	−9	0.72				
			−54	27	3	0.68				
Inferior frontal gyrus (F3op)	44	R					39	12	27	0.59
							54	15	30	0.55
Precentral sulcus (PrCS)	8	R					36	6	45	0.76
							45	27	45	0.75
							42	36	21	0.69
Superior frontal gyrus	9/8	M	−3	33	39	0.72	−6	30	45	0.80
			0	48	39	0.65				
		R					15	30	45	0.63
Supplementary motor area	6	M					−6	9	54	0.66
Middle temporal gyrus	21/37	R					54	−42	0	0.62
							66	−42	−6	0.53
Supramarginal gyrus	40	L	−54	−48	33	0.77				
		R					36	−57	36	0.65
Inferior parietal gyrus	7	L					−54	−39	51	0.77
							−39	−57	57	0.76
		R					51	−36	51	0.75
							39	−48	51	0.71
Superior parietal gyrus	7	L					−21	−72	57	0.70
		R					36	−57	60	0.70
							18	−72	51	0.63
Precuneus	7/31	M					−12	−72	63	0.63
							−6	−69	51	0.62
Cingulate gyrus	23/31	M					12	−36	42	0.61

Note. Stereotactic coordinates (*x*, *y*, *z*) in MNI space are shown for each voxel with a local maximum of correlation coefficients ($r > 0.5$) in the S or P tasks under the auditory and visual conditions merged. For each region in each hemisphere, at most three local maxima are indicated.

as ROIs (Figs. 2A and D). The spatial extents of these ROIs were determined by the voxels activated in either S_A–P_A or S_V–P_V. For both L. F3t/F3O and L. PrCS, the time courses of individual voxels were highly correlated with an averaged time course in each ROI ($r > 0.5$ for most voxels), suggesting that it is representative of signal changes during the S tasks in the whole ROI (Figs. 2B and E). In contrast, the time courses of individual voxels showed weaker correlations with the time course of a local maximum in each ROI during the S tasks [L. F3t/F3O: (−48, 24, −9) and L. PrCS: (−42, 24, 48); Figs. 2C and F], which was determined in the overlapped region under both auditory and visual conditions. Therefore, we adopted in the subsequent analyses the averaged time courses as best representing the overall activation of the defined ROI.

Temporal correlations related to sentence processing

We examined the pattern of temporal correlations of each ROI with other cortical regions during a specific language task. For each ROI, we found that the correlation patterns were markedly different according to the types of the tasks employed. During the S tasks, L. F3t/F3O showed significant correlations with cortical regions in the left hemisphere, including L. PrCS as the most prominent region of correlations, as well as L. SMG and the medial surface of the superior frontal gyrus (Fig. 3A and Table 3). These correlations were replicated in separate analyses for either S_A (Fig. 3B) or S_V (Fig. 3C) blocks. In contrast, during the P tasks, L. F3t/F3O showed the most prominent correlation with the right F3t/F3O in addition to the left superior temporal gyrus (Fig. 3D), which were consistent

with separate analyses for either P_A (Fig. 3E) or P_V (Fig. 3F) blocks. These results were basically consistent when L. PrCS was chosen as a reference region of correlation. During the S tasks, L. PrCS was correlated mostly with cortical regions in the left hemisphere, including L. F3t/F3O and L. SMG (Figs. 3G–I). During the P tasks, in contrast, cortical regions exhibiting significant correlation with L. PrCS were distributed equally in both hemispheres, with prominent regions including the right PrCS, as well as the inferior and superior parietal gyri (Figs. 3J–L). These results clearly demonstrate that the functional connectivity between L. F3t/F3O and L. PrCS does not depend on input modalities of audition and vision, i.e., it is basically amodal. In the following analyses, we thus used the merged data between the input modalities in each of the S and P tasks.

The correlation patterns observed in Fig. 3 clearly demonstrate the selective enhancement of the reciprocal connectivity between L. F3t/F3O and L. PrCS in the S tasks, but not in the P tasks. To confirm this sentence-selective enhancement quantitatively, we performed a ROI analysis by examining the distribution of correlation values within the extent of each ROI for S or P tasks. With respect to L. F3t/F3O as a reference region, we found that 67% and none of the voxels in L. PrCS exhibited significant correlation above the threshold ($r > 0.5$) for the S and P tasks, respectively (Fig. 4A). For both tasks, the pattern of the correlations was characterized by a distribution with a single peak, but with no additional peaks in its tail. A Mann–Whitney test revealed that the difference in the distributions was highly significant between the two tasks ($P < 0.0001$). Similarly, with respect to L. PrCS as a reference region, we found that 62 and 2% of the voxels in L. F3t/F3O showed significant correlations for the S and P tasks, respectively, with highly significant differences between the distributions ($P < 0.0001$). Therefore, the ROI analyses presented here confirmed that L. F3t/F3O and L. PrCS exhibit selective enhancement in their correlations during sentence processing.

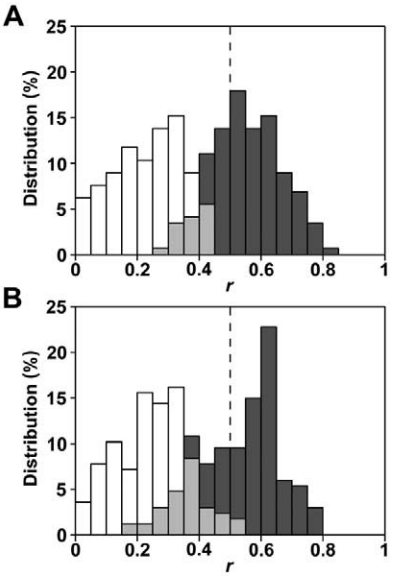

Fig. 4. The difference in distributions of correlation coefficients between the S and P tasks. (A) Histograms represent the distributions of correlation coefficients between the time course of the voxels in L. PrCS and an averaged time course in L. F3t/F3O as a reference region. The dark gray and white bars denote the fraction of the voxels that exhibited correlation coefficients during the S and P tasks, respectively, whereas the light gray bars denote overlaps between the dark gray and white bars. (B) Histograms represent the distributions of correlation coefficients between the time course of the voxels in L. F3t/F3O and an averaged time course in L. PrCS as a reference region. The distributions for the S and P tasks are clearly separated.

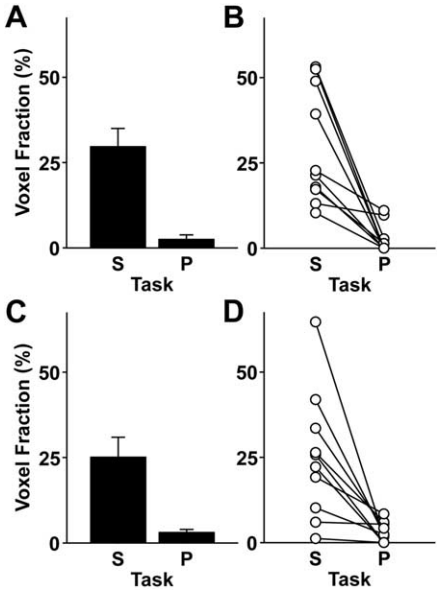

Fig. 5. Individual analyses for temporal correlations between L. F3t/F3O and L. PrCS. (A) Each bar represents the voxel fraction in L. PrCS that exhibited significant correlations ($r > 0.5$) with L. F3t/F3O as a reference region, as measured on a subject level (mean ± standard errors of subjects, $N = 10$). (B) The same voxel fractions in (A) are shown for each individual (circles with a line). (C and D) The same as (A) and (B), but the voxel fractions in L. F3t/F3O that exhibited significant correlations with L. PrCS as a reference region are shown.

We next performed individual analyses treating subjects as a random effect. For each subject in each task, we evaluated temporal correlations between L. F3t/F3O and L. PrCS (the same regions in the normalized brains) and performed a ROI analysis by counting the number of voxels that exhibited significant temporal correlations ($r > 0.5$). We found that the features observed in Figs. 3 and 4 were well preserved on a subject level as well. In Fig. 5A, the bars indicate the mean voxel fraction in L. PrCS that exhibited significant correlations with L. F3t/F3O as a reference region. A paired t test confirmed that the temporal correlations of L. PrCS with respect to L. F3t/F3O were significantly different between the S and P tasks ($t = 4.6$, $P < 0.002$), indicating that the connection of the two regions is strengthened significantly during sentence processing. Likewise, we confirmed that the temporal correlations of L.

F3t/F3O with respect to L. PrCS as a reference region were significantly different between the S and P tasks (Fig. 5B; $t = 3.7$, $P < 0.005$). We therefore conclude that the functional connectivity between L. F3t/F3O and L. PrCS is selectively enhanced during sentence processing.

These findings are consistent with our previous studies, in that L. F3t/F3O was selectively involved in sentence-related processes beyond lexical processing (Homae et al., 2002). They are also consistent with our hypothesis that the L. F3t/F3O is involved in the selection and integration of lexico-semantic information based on syntactic structures and that L. DPFC, which is close to L. PrCS, is specifically involved in syntactic processing (Hashimoto and Sakai, 2002). Therefore, we further hypothesize that the cortico-cortical pathway within the left prefrontal cortex subserves the use of syntactic information for integrating lexico-semantic information. Because semantic interpretation of sentences is clearly dependent on syntactic information, this integration process is crucial in sentence comprehension (Smith and Wilson, 1979). One theoretical model has proposed an initial stage for building syntactic structures on the basis of word-category information, and a later stage for integration of syntactic and lexico-semantic information (Frazier, 1987). In contrast, another model has assumed an interaction between syntactic and lexicosemantic processes from an early stage (Marslen-Wilson and Tyler, 1980). Both models postulate that syntactic and lexico-semantic information is integrated in the course of sentence processing, which may subsist in the functional network of the left prefrontal cortex.

Conclusions

We found that two regions in the left prefrontal cortex, L. F3t/F3O and L. PrCS, exhibited selective enhancement in their reciprocal functional connectivity during sentence processing. Because the analyses accounted for sentence processing under both auditory and visual conditions, the results would reflect the amodal aspects of corticocortical connectivity during language processing. Moreover, we found that the patterns of temporal correlations were substantially different according to the levels of language processing. During the tasks requiring lexical level decisions, functional connections extended over both hemispheres, whereas during the tasks requiring sentence level comprehension, the connections were mostly lateralized to the left hemisphere. The present study suggests that functional connectivity in the cerebral cortex changes dynamically according to a specific component of linguistic processes.

Acknowledgments

We thank R. Hashimoto, Y. Hashimoto, and Y. Noguchi for their technical assistance, and H. Matsuda for her administrative assistance. This study was supported by a Solution Oriented Research for Science and Technology (SORST) grant from Japan Science Technology Corporation and by a Young Investigator's Grant from Human Frontier Science Program (HFSP) awarded to K.L.S.

References

Bokde, A.L.W., Tagamets, M.A., Friedman, R.B., Horwitz, B., 2001. Functional interactions of the inferior frontal cortex during the processing of words and word-like stimuli. Neuron 30, 609–617.

Catani, M., Howard, R.J., Pajevic, S., Jones, D.K., 2002. Virtual in vivo interactive dissection of white matter fasciculi in the human brain. Neuroimage 17, 77–94.

Conturo, T.E., Lori, N.F., Cull, T.S., Akbudak, E., Snyder, A.Z., Shimony, J.S., McKinstry, R.C., Burton, H., Raichle, M.E., 1999. Tracking neuronal fiber pathways in the living human brain. Proc. Natl. Acad. Sci. USA 96, 10422–10427.

Embick, D., Marantz, A., Miyashita, Y., O'Neil, W., Sakai, K.L., 2000. A syntactic specialization for Broca's area. Proc. Natl. Acad. Sci. USA 97, 6150–6154.

Frazier, L., 1987. Sentence processing: a tutorial review, in: Coltheart, M. (Ed.), Attention and Performance XII — The Psychology of Reading, Erlbaum, London, pp. 559–586.

Friston, K.J., Frith, C.D., Liddle, P.F., Frackowiak, R.S.J., 1993. Functional connectivity: the principal-component analysis of large (PET) data sets. J. Cereb. Blood Flow Metab. 13, 5–14.

Gonçalves, M.S., Hall, D.A., Johnsrude, I.S., Haggard, M.P., 2001. Can meaningful effective connectivities be obtained between auditory cortical regions? Neuroimage 14, 1353–1360.

Hampson, M., Peterson, B.S., Skudlarski, P., Gatenby, J.C., Gore, J.C., 2002. Detection of functional connectivity using temporal correlations in MR images. Hum. Brain Mapp. 15, 247–262.

Hashimoto, R., Sakai, K.L., 2002. Specialization in the left prefrontal cortex for sentence comprehension. Neuron 35, 589–597.

Hays, W.L., 1994. Statistics. Harcourt Brace College, Fort Worth, TX.

Homae, F., Hashimoto, R., Nakajima, K., Miyashita, Y., Sakai, K.L., 2002. From perception to sentence comprehension: the convergence of auditory and visual information of language in the left inferior frontal cortex. Neuroimage 16, 883–900.

Horwitz, B., Grady, C.L., Haxby, J.V., Schapiro, M.B., Rapoport, S.I., Ungerleider, L.G., Mishkin, M., 1992. Functional associations among human posterior extrastriate brain regions during object and spatial vision. J. Cog. Neurosci. 4, 311–322.

Marslen-Wilson, W., Tyler, L.K., 1980. The temporal structure of spoken language understanding. Cognition 8, 1–71.

Oldfield, R.C., 1971. The assessment and analysis of handedness: The Edinburgh inventory. Neuropsychologia 9, 97–113.

Poupon, C., Clark, C.A., Frouin, V., Régis, J., Bloch, I., LeBihan, D., Mangin, J.F., 2000. Regularization of diffusion-based direction maps for the tracking of brain white matter fascicles. Neuroimage 12, 184–195.

Sakai, K.L., Noguchi, Y., Takeuchi, T., Watanabe, E., 2002. Selective priming of syntactic processing by event-related transcranial magnetic stimulation of Broca's area. Neuron 35, 1177–1182.

Smith, N., Wilson, D., 1979. Modern Linguistics: The Results of Chomsky's Revolution. Indiana Univ. Press, Bloomington.

Suzuki, K., Sakai, K.L., 2003. An event-related fMRI study of explicit syntactic processing of normal/anomalous sentences in contrast to implicit syntactic processing. Cereb. Cortex 13, 517–526.

Tzourio-Mazoyer, N., Landeau, B., Papathanassiou, D., Crivello, F., Etard, O., Delcroix, N., Mazoyer, B., Joliot, M., 2002. Automated anatomical labeling of activations in SPM using a macroscopic anatomical parcellation of the MNI MRI single-subject brain. Neuroimage 15, 273–289.